INTERNATIONAL JOURNAL OF AUTOMOTIVE AND MECHANICAL ENGINEERING (IJAME)
ISSN: 2229-8649 e-ISSN: 2180-1606
VOL. 17, ISSUE 1, 7524 – 7532
DOI: https://doi.org/10.15282/ijame.17.1.2020.01.0556

ORIGINAL ARTICLE

Performance Study of RTV-2 Silicone Rubber Material for Soft Actuator: The Effect of Inflation Pressure and Wall Thickness

Deepak D[1*], Nitesh Kumar[1], Shreyas P Shetty[1], Saurabh Jain[1], Manoj Bhat[2]

[1]Department of Mechanical and Manufacturing Engineering, Manipal Institute of Technology, Manipal Academy of Higher Education, India
Phone: Ph:91-7204308289
[2]Department of Mechanical Engineering, Carnegie Mellon University, U.S.A.

ABSTRACT – The expensive nature of currently used materials in the soft robotic industry demands the consideration of alternative materials for fabrication. This work investigates the performance of RTV-2 grade silicone rubber for fabrication of a soft actuator. Initially, a cylindrical actuator is fabricated using this material and its performance is experimentally assessed for different pressures. Further, parametric variations of the effect of wall thickness and inflation pressure are studied by numerical methods. Results show that, both wall thickness and inflation pressure are influential parameters which affect the elongation behaviour of the actuator. Thin (1.5 mm) sectioned actuators produced 76.97% more elongation compared to thick sectioned, but the stress induced is 89.61 % higher. Whereas, the thick sectioned actuator (6 mm) showed a higher load transmitting capability. With change in wall thickness from 1.5 mm to 6 mm, the elongation is reduced by 76.97 %, 38.35 %, 21.05 % and 11.43 % at pressure 100 kPa, 75 kPa, 50 kPa and 25 kPa respectively. The induced stress is also found reduced by 89.61 %, 86.66 %, 84.46 % and 68.68 % at these pressures. The average load carrying capacity of the actuator is found to be directly proportional to its wall thickness and inflation pressure.

ARTICLE HISTORY
Revised: 3rd June 2019
Accepted: 19th Dec 2019

KEYWORDS
Soft actuator, RTV-2 Silicone rubber, Yeoh model, Hyperelastic material, Elongation, Load transmitted, Flexible actuators.

INTRODUCTION

Soft actuators are developed by using flexible materials like elastomers, hydrogels, and shape memory alloys, etc. Major applications of the same available in the literature are for grasping and moving of light objects, medical rehabilitation through artificial limbs and shoulders [1], rehabilitation belt [2], invasive surgical applications [3] and for exoskeletons [4]. This technology is gaining rapid attention in the research community. The potential fields of research are the development of co-robots, self-healing and replicating robots for locomotion in rough terrains and marine applications.

Ganesha et al. [5] studied the effect of geometrical variation in single-chambered asymmetric actuators on bending and gripping force. Increase in pressure up to 120 kPa resulted in deflection of actuator up to an angle of 37º, further increase in pressure (up to 180 kPa) resulted in bending with a radius of curvature (56º). The gripping force was increased linearly with the pressure. Similar trends were observed in numerical simulations, but the gripping force determined by the experimental method was higher. Robertson et al. [6] studied the effect of packing of multiple actuators with different configurations on the gripping force. The packed actuators were found to produce a higher linear force (112 N) compared to non-packed actuators. The actuator with reinforcements like glass spheres and polyaramid fabric increased its mechanical strength and load-carrying capacity up to 8 kg [7]. Feng Ni et al. [8] developed soft jumping robots in which the desired directional jump was obtained by the variable timing of leg actuation. Andrew D. Marchese et al. [9] made a comparative characterisation of actuators having ribbed, cylindrical and pleated segments. The study shows that the maximum stiffness of 60 kPa was exhibited by the pleated type actuator compared to other configurations. To track the actuator motion as well as the pressure distribution and the corresponding force transmitted by the actuators, flex sensors were embedded [10-12]. The sensor feedback was used to understand the bending behaviour of the actuator and to predict its deformation. This enabled building artificial intelligence in the robots for better interaction with the environment.

Panagiotis Polygerinos et al [13] studied the effect of wall thickness (up to 12 mm) and actuating pressure on its bending angle through simulations. These results were experimentally validated by an actuator made of Elastosil M4601. The increase in wall thickness required higher inflation pressure for bending the actuator (for angles of 900, 1800 and 3600). Also, the force exerted at the tip of the actuator was increased with the decrease in length of the actuator. Yahya Elsayed et al [14] investigated the performance of Ecoflex 0030, 0050 and Dragonskin 0030 elastomers with different cross-sections namely circular, semi-circular, circular-sector and ring-sectored. The Ecoflex 0050 actuator was found to sustain higher pressure (0.32 bar) compared to other elastomeric materials for producing the same amount of bending. The von-Mises pressure of the Ecoflex 0050 (9 x 106 Pa) was greater than Exoflex 0030 (3 x 106 Pa). In ring-type design, the balloon-projected area was decreased with an increase in the area of the chamber. The actuators having semi-circular design showed the smallest balloon area.

*CORRESPONDING AUTHOR | Deepak D. | ✉ deepak.d@manipal.edu

Philip Moseley et al. [15] studied the performance of soft rodent exoskeleton and hand rehabilitation glove made by Ecoflex 0030 for different loading conditions. At a pressure of 40 kPa, the strain observed was 600%, the free displacement was 70 mm and the actuator force was 5.66 N. G. Runge [16] developed an FEM based kinematic modelling framework to capture the non-linear behaviour of the soft actuator. Piecewise constant curvature approach with hyper-elastic Yeoh model was used for the numerical modelling. The experimental validation was made with Ecoflex 0050 silicone material. Study shows that the increase in the length of actuator resulted in higher deflection at any input pressure (220 mbar and 230 mbar). The actuators of shorter lengths required higher pressure compared to longer actuators to obtain the same amount of deflection.

Frederick Largilliere [17] developed a model which produced a generic solution to control the soft actuators with real-time constraints based on results of FEM for obtaining the desired trajectory. Yufei Hao et al [18] studied the influence of the top wedged angle on bi-directional bending using dragon-skin 30 in which the effect of material combinations and actuator widths were simulated. The material softness and the wedge angle showed significant influence on the bending of the actuator. The actuator with greater width deformed easily and produced a greater gripping force. It was found that, no significant difference in the bending angle observed in amphibious condition compared to open air. Maria Pozzi et al [19] studied the torsional and bending stiffness obtained at various pressures for predicting the deformation path using three-layered simulation framework. In a very short computational time, this method produced a result which was closer to the actual deformation compared to the results estimated by conventional simulation approach. Kit Hang Lee [20] developed a control framework to characterise the kinematics of soft robotics through hyper-elastic finite element modelling. This model used Jacobian mapping to capture the user input and the end effector output.

Intra-cavity motion modelling was made for simulations and the results were validated by experiments. Guanjun Bao et al [21] developed pneumatic trunk-like soft actuator which had independent chambers for driving and stiffness adjustment. The theoretical models were established to describe the elongation and bending motion of the actuators. Major challenges in the field of soft robotics are dexterous motion, proprioceptive sensing and robust control of its deformable bodies during the interaction of its actuators with the environment. Wenbin Chen et al [22] proposed to embed a curvature proprioceptive sensor in actuators for determining the bending profile. The sensor data was used to develop a differential equation that describes the nonlinear behaviour of the soft actuator. Renato Gasoto et al [23] proposed a constraint-based dynamics model of a 1-dimensional pneumatic soft actuator considering the internal pressure forces, the effect of actuator latency and damping under inflation and deflation. Weiping Hu et al [24] investigated the effects of design parameters on the actuation performance of a pneunet actuator and made structural optimization using the finite element method (FEM). The effects of the structural parameters such as operation pressure, the wall thickness and the gap between the chambers, bottom layer thickness, and the geometry of the channel cross-section on the deformation and bending angle of the actuator. The bending angle was found to be decreased with the increase in wall thickness. The actuator having round cross-section showed lower radius of curvature in bending compared to rectangular, half rounded and honeycomb cross-sectioned actuators. Ramin Zakeri et al [25] simulated dissipative particle dynamics of the soft micro-actuator using polymer chain displacement in electro-osmotic flow. The results showed that the displacement rate can be increased by increasing the electric field. Zhou et al [26] performed FEM simulations to precisely predict the electromechanical behaviours of the dielectric elastomer-based soft actuator. With the optimal design, the finger-like soft actuator generated large deflections with the bending angle about of 128°.

In general, soft actuators are fabricated by 3D printing or conventional moulding methods. To provide multiple degrees of freedom, each actuator is fabricated with multiple air chambers which are inflated by compressed air. The path traced by the actuator in space depends on the air pressure in different chambers and its material properties. D Deepak et al. [27] explored the possibility of using natural rubber for developing the soft actuator. The actuator made of natural latex developed pores within due to the expulsion of water. The use of additive such as formic acid reduced this limitation. Determination of actuator path produced by various materials using experimental methods is expensive. In this scenario, the FEM simulations are affordable to understand the actuator kinematics for different materials and conditions. This work attempts to use the numerical methods to explore the elongation behaviour and the load transmitted by the soft actuator fabricated by RTV-2 silicone rubber. The simulated results are validated with the experimental work. In the absence of comprehensive methods for design and modelling of the soft actuators, this work provides a suitable framework for the design of soft actuators.

METHODOLOGY

This work investigates the effect of actuator wall thickness, inflation pressure and wall thickness to actuator diameter (t/d) ratio on longitudinal elongation, maximum stress developed on the actuator and its load transmitting capacity. The following section details the fabrication process of the actuators, the experimental setup to determine the inflation process and the numerical modelling of the computational domain.

Fabrication of Actuators

The material used for fabrication of actuator is RTV-2 silicone rubber (supplied by Aditya Silicone) and its properties are shown in Table 1. The mould for the actuator was prepared by a fused deposition-based 3D printer (make: Fractal Works, model: Julia) using acrylonitrile butadiene styrene (ABS) filaments. Figure 1 shows various stages of the actuator fabrication process. The elastomer was mixed with a catalyst AD-1/B in the ratio 10:1 at room temperature. The elastomer mixture is then slowly poured into the mould. The pouring rate of the elastomer mixture was carefully controlled to

evacuate the bubbles formation. Initially, the actuator is cured at room temperature for 4 hours and then post-cured at a temperature of 80 ºC for 2 hours as specified by the elastomer manufacturer.

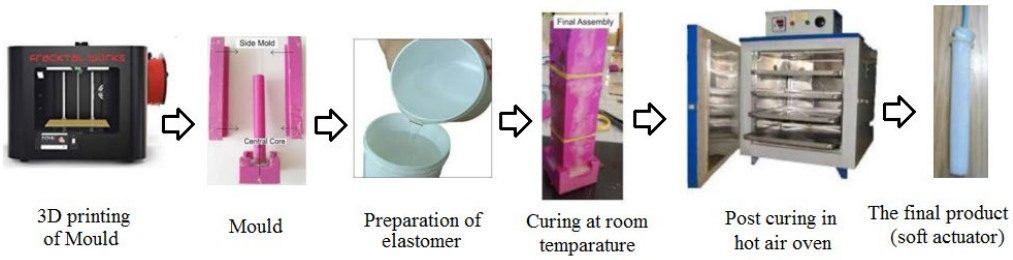

Figure 1. Fabrication of actuator.

Table 1. Properties of RTV-2 silicone rubber.

Pot Life	Viscosity	Density	Elongation
60 min	30,000 cps	1070 kg/m^3	650%

Experimental Setup

Figure 2 shows the experimental setup which was developed in-house to assess the performance of the actuator. The compressor operates at 12 V and generates an airflow of 33.33 ml/s at a maximum pressure of 100 kPa. First, compressed air is supplied to the actuator and its corresponding inflation was digitally recorded using a DSLR camera (make: Nikon, model: D5500). In the background of the actuator, a paper sheet with standard grids is placed to measure inflation. The recorded data is processed using digital image processing software. The frames that were captured during inflation of actuator at different timings were extracted from the video file. Using these frames, the percentage strain along the axis of the actuator was calculated.

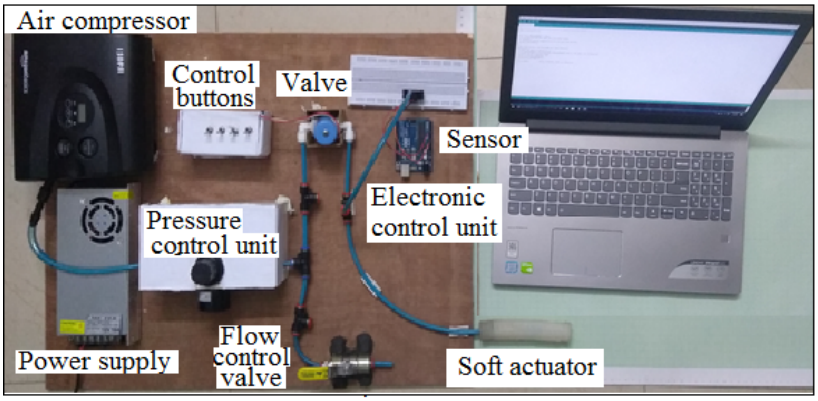

Figure 2. Experimental setup.

Modelling of Computational Domain

The meshing of the computational domain was carried out by using the multi-zone hybrid meshing method. Considering the geometry of the model, a combination of hexahedral and tetrahedral elements with an optimum mesh size of 6,55,498 elements were used for meshing at appropriate locations. The meshed model and the boundary conditions imposed for the simulations are shown in Figure 3. The correlation of experimental stress-strain data with Yeoh second-order hyperelastic model from Eq. (1) is shown in Figure 4. There is a good agreement of the data, and hence, the same model was adopted in numerical modelling for capturing the elongation behaviour of actuator.

The engineering stress in Eq. (3) was calculated using Cauchy stress in Eq. (4) which can be related to the pressure applied for obtaining the principal engineering strain values.

$$U(I_1, I_2) = C_{10}(I_1 - 3) + C_{20}(I_2 - 3)^2 + \frac{1}{d_1}(J-1)^2 + \frac{1}{d_2}(J-1)^4 \quad (1)$$

$$d_1 = d_2 = \frac{2}{K} = 0.299e^{-5} \quad (2)$$

$$s = \frac{\sigma}{1+\epsilon} \quad (3)$$

$$\sigma = -p + 2\alpha^2 \frac{\partial U}{\partial I} \tag{4}$$

Where, U - Energy function, I_1 and I_2 - deviatoric first and second principal invariant, J- Jacobian, d - incompressibility parameter (Equation. 2), k - bulk modulus, σ - resultant stress, s and $\dot{o}$ are engineering stress and strain respectively, and the stretch ratio $\alpha = 1 + \varepsilon_{eng\ strain}$.

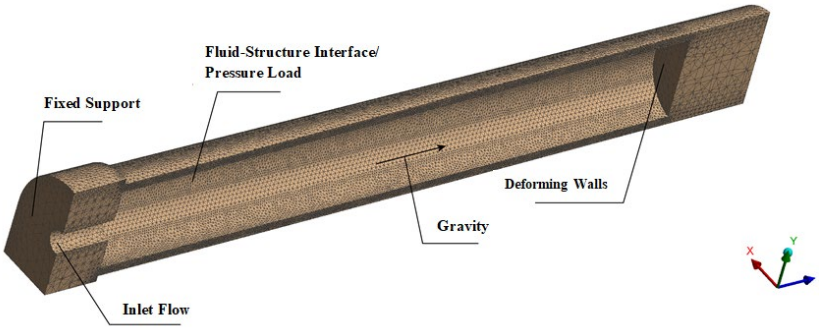

Figure 3. Computational domain with boundary conditions.

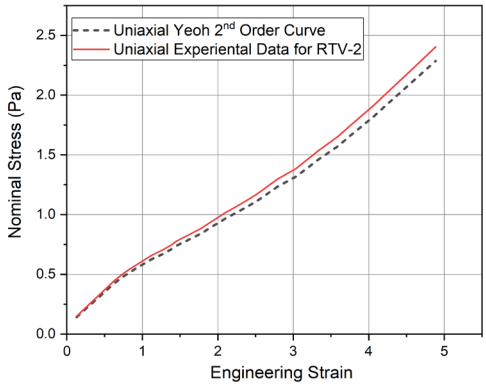

Figure 4. Stress-Strain curves of the chosen model and experimental data.

The non-linear effects and large deformations were also considered in the model. The self-contact regions are chosen as frictional with coefficient 0.2. The pure penalty is adopted to improve the convergence at contact regions and the stiffness damping is set to 0.2 for faster convergence. Gravitational acceleration load is considered and the pressure is ramped to a maximum pressure of 100 kPa for 10 s. For the time frame of the 20 s, the maximum pressure developed is 60 kPa. Force convergence equations are solved by decreasing the residuals between the external and internal loads. Due to structural non-linearity of the material, geometrical change of the computational domain is expected as pressure developed inside the actuator. Two-way coupling of force loads formed fluid flow and displacement of the transient structure. The turbulence is modelled using a Realizable k-ε model with scalable wall function as developed by Launder and Spalding [22]. Re-meshing and smoothing of control volume mesh were used for convergence of the solution. To reduce the complexity of the computational effort, element-wise varying loads were approximated to a pressure load which is acting on the inner surface of the actuator. The profiles of the pressure load were approximated to be linear.

RESULTS AND DISCUSSION

Validation of Numerical Simulations

The actuator is inflated by compressed air and the corresponding deformation is recorded using a high-resolution camera. The pressure developed inside the actuator is precisely monitored using the pressure sensors (make: MPX5010). Figure 5 (a) shows the deformation of the actuator at different time interval for the duration of 20 s at an inflation pressure of 100 KPa. With similar conditions, the numerical simulations were also performed and its corresponding axial elongation is shown in Figure. 5 (b) along with experiments results. It is observed that there is a good agreement in axial elongation of the actuator with a maximum error of 14.49 %.

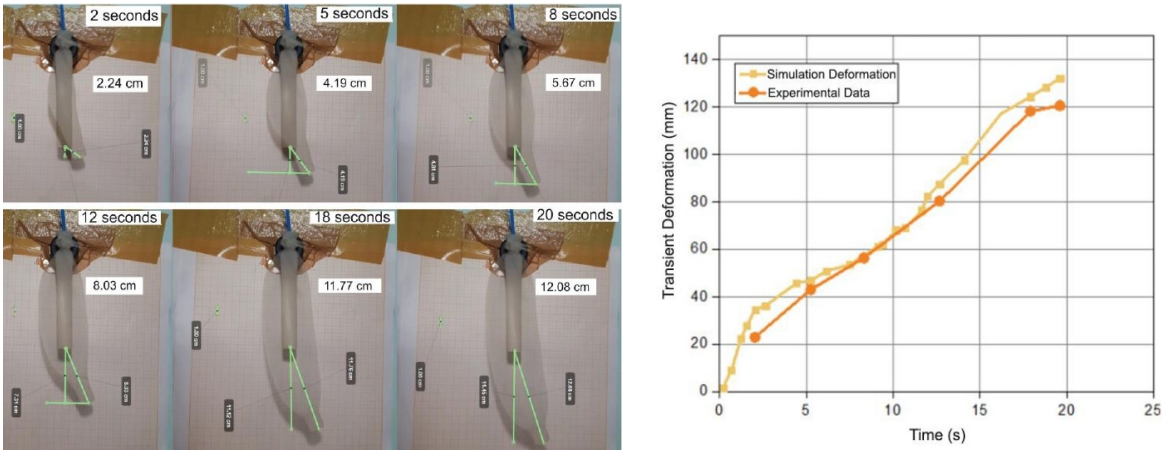

(a) (b)

Figure 5. (a) Actual deformation and (b) elongation in experimental and numerical simulations at 100 kPa pressure.

The Effect of Wall Thickness

Rubber actuators of wall thickness varying from 1.5 mm to 6 mm were subjected to the inflation pressure of 25 kPa to 100 kPa. The corresponding temporal wall deformation (axial elongation) obtained by the numerical simulation is shown in Figure 6. It is observed from Figure 6 (a) that for a wall thickness of 1.5 mm, at any applied inflation pressure, initially, the deformation appears to be increasing linearly for a short period and then it increases almost exponentially.

Figure 6 (b) to 6 (d) shows similar trends for actuators of different wall thickness. According to Mullin's effect [28], the initial linear variation is due to the higher material stiffness. The continued loading led to an exponential variation of deformation due to strain-induced stress softening of actuator material. Further, it is observed from these figures that, the increase in wall thickness resulted in decreasing deformation. Interestingly, the rate of deformation changed from exponential to almost linear behaviour for actuators of higher wall thickness. This is due to higher stiffness of the actuator wall which results in reducing the deformation.

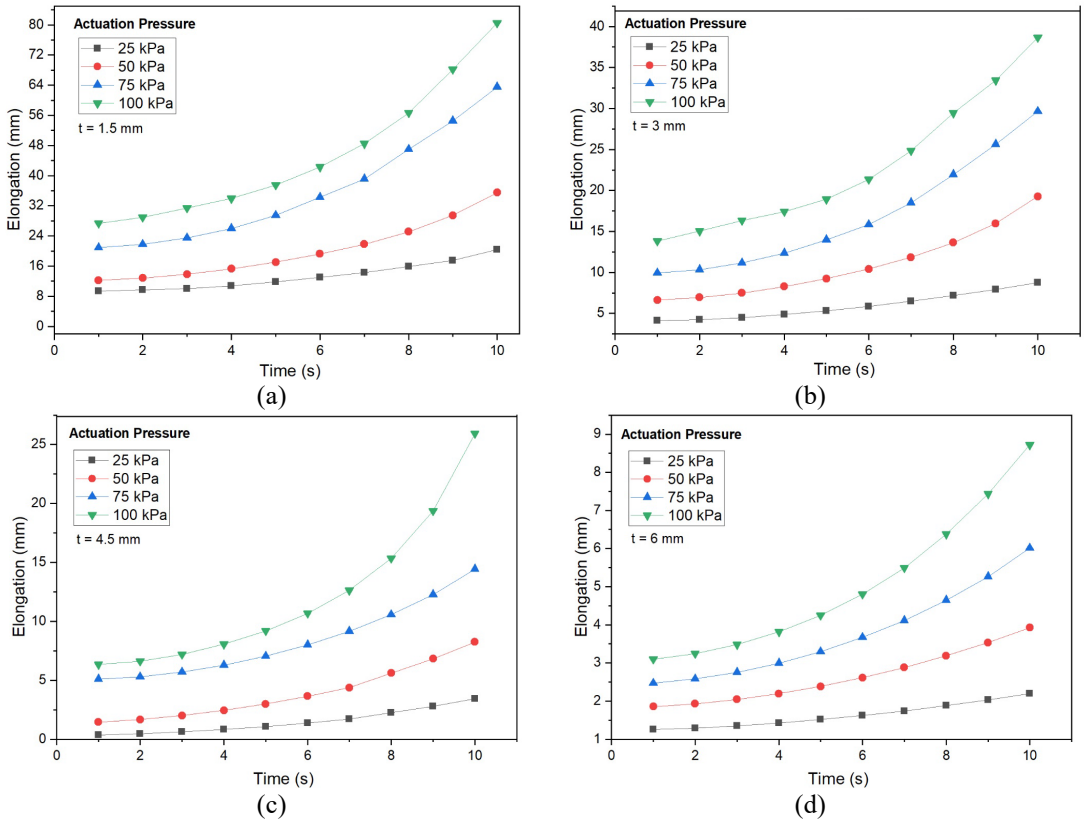

(a) (b) (c) (d)

Figure 6. Effect of actuator wall thickness on elongation (a) t = 1.5 mm, (b) t = 3 mm, (c) t = 4.5 mm and (d) t = 6 mm.

The Effect of Inflation Pressure

The effect of wall pressure on the longitudinal deformation (axial elongation) of the actuator of various thicknesses is shown in Figure 7(a) to 7(d). For actuators of any wall thickness, the increase in inflation pressure resulted in an increase

of longitudinal elongation. Interestingly, at lower inflation pressure, the elongation is linear for all actuators (wall thickness of 1.5 mm to 6 mm).

When the pressure was increased from 25 kPa to 75 kPa, there is a transition of linear to non-linear elongation. For an increase of pressure from 75 kPa to 100 kPa a non-linear elongation is observed for the actuators of wall thickness up to 4.5 mm. This is due to the elastic behaviour of the elastomer which initially deforms relatively with a lower yield with respect to time in accordance with Yeoh second-order model. At higher pressures, a deviation from the Yeoh second-order model is observed as it does not consider the pressure-induced gain within the material which induce non-linear exponential deviation within a short interval. But, beyond wall thickness of 4.5 mm, a linear elongation is observed. This is due to the increase in material stiffness which leads to a lower elongation rate. It is also evident from the stress plots shown in Figure 7 that, for a wall thickness of 1.5 mm the stress is linear at a pressure of 25 kPa and it becomes non-linear beyond this pressure. For wall thickness of 3 mm and 4.5 mm, the induced stress becomes non-linear at a pressure of 75 kPa and 100 kPa respectively. But, for a wall thickness of 6 mm, the induced stress is linear at all inflation pressures. The actuators that have thinner cross-sections seemingly exhibit elongation in accordance with Yeoh second-order models as evident from Figure. 7(a) (for actuator of 1.5mm thickness). This phenomenon was also exhibited by the thicker actuators at higher pressures. This behaviour can help the researchers in determining the thickness of the actuators to be used in the experiments in order to get the desired results. As evident from Figure. 7(d), the linear characteristics for the actuator of thickness 6 mm, the 100 KPa pressure indicate that actuators of larger thickness are not suitable for soft actuation as it completely deviates from Yeoh model predictions.

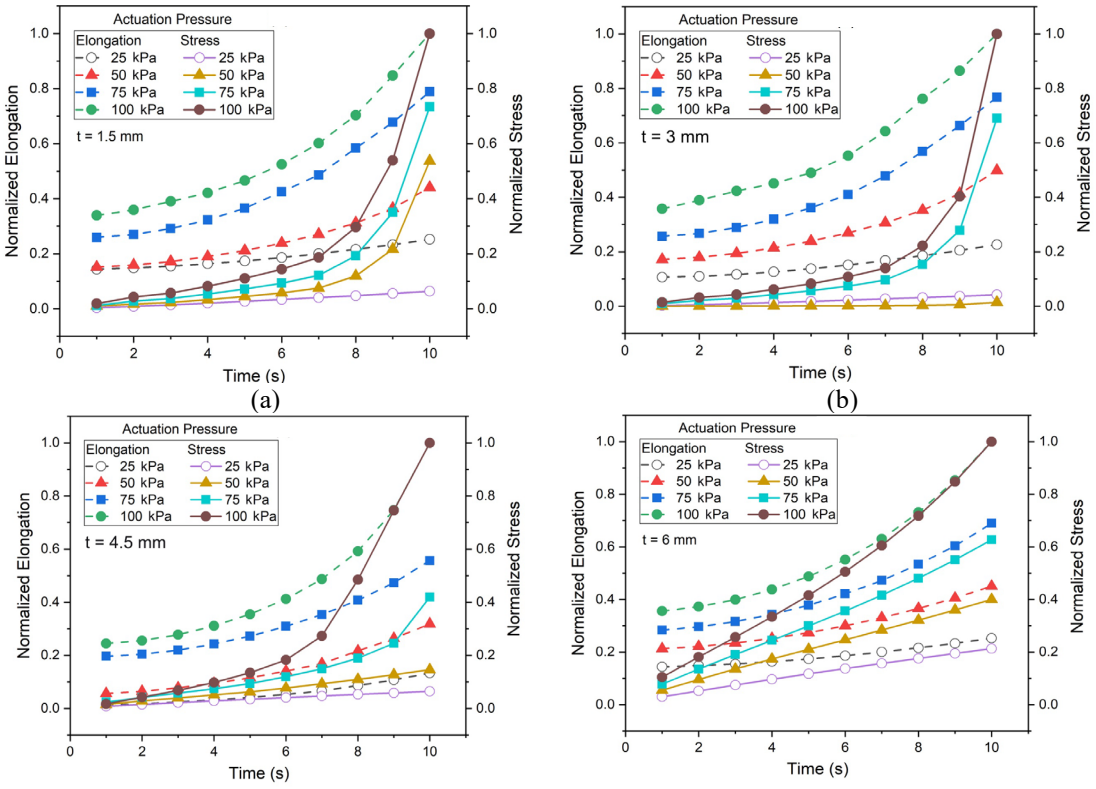

Figure 7. Effect of inflation pressure on elongation and stress for wall thickness of (a) t = 1.5 mm, (b) t = 3 mm, (c) t = 4.5 mm and (d) t = 6 mm.

The Effect of Wall Thickness and Actuator Diameter (t/d) Ratio

Figure 8(a) and 8(b) show the maximum elongation and the corresponding stress developed for actuators of various t/d ratios. Figure 9(a) and 9(b) show the contour plot Von-Mises stress and elongation of the actuator at different time intervals respectively. Both elongation and stress developed in the actuator were found to decrease with increase in t/d ratio. This is due to the increase in stiffness of actuator with an increase in wall thickness. The maximum stress (Von-Mises stress) is at the midway of the actuator as shown in Figure 9(a) where the inflation of the actuator reduces the thickness at the midway belly to a minimum and hence maximum stress is developed. Figure 9(b) shows the directional elongation of the actuator shows a maximum directional displacement of 90.164 mm in the direction of application of inlet pressure.

At the lower t/d ratio, the elongation of the actuator changes from 20% to 57% of the original length for change in pressure from 25 kPa to 100 kPa. With the increase in t/d ratio, this difference reduced gradually as shown in Table 2. At a t/d ratio of 0.4 there is a drastic reduction in elongation (less than 12.7 %) even at high inflation pressures. The corresponding maximum stress developed at different t/d ratio is shown in Table 3.

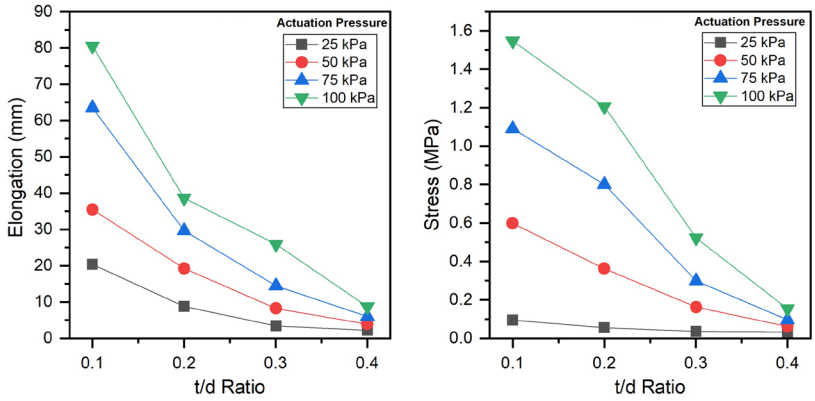

(a) (b)

Figure 8. Effect of inflation pressure on (a) elongation and (b) stress.

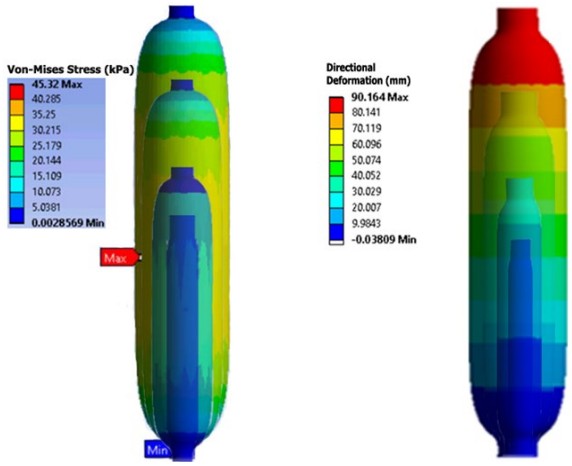

(a) (b)

Figure 9. (a) Von-Mises stress and (b) elongation plot of the actuator at different time intervals.

Table 2. Axial elongation of the actuator.

t/d ratio	Wall thickness	Inflation pressure (kPa)			
		25	50	75	100
0.1	1.5 mm	27.01	39.58	62.94	77.11
0.2	3.0 mm	17.29	26.05	34.70	42.21
0.3	4.5 mm	10.88	12.69	22.04	31.62
0.4	6.0 mm	10.73	13.27	15.00	17.26

Table 3. Maximum equivalent stress developed.

Wall thickness	25 kPa	50 kPa	75 kPa	100 kPa
1.5 mm	93.23	550.53	1093.4	1482.94
3.0 mm	53.12	553.58	934.44	1298.51
4.5 mm	33.64	92.54	243.36	524.54
6.0 mm	29.34	85.22	91.45	154.54

The Load Transmitting Capacity

The maximum axial load carrying capacity of an actuator with different thicknesses and inflation pressure is shown in Figure 10. It is observed that, for any chosen actuators, its load-carrying capacity increased with an increase in inflation pressure as well as its wall thickness. Due to the increase in pressure from 25 kPa to 100 kPa and change in wall thickness from 1.5 mm to 6 mm, the average load transmitting capacity of the actuator is proportionally increased by 247.92 % and 345.08 % respectively. But, the higher wall thickness in actuator always limits the length of elongation as shown in Figure 8. In addition, the higher loads on the actuator resulted in bulging of actuator laterally instead of transmitting the load along its axis. The maximum load displaced by the actuator of thicknesses 1.5 mm and 6 mm is 1.63 N and 6.42 N respectively (at pressure: 100 kPa). Table 4 gives the load transmitting capacity of the actuators obtained at varying pressures.

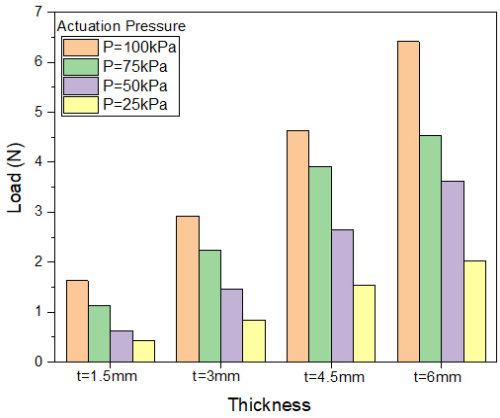

Figure 10. Load transmitting capacity of the actuator.

Table 4. Load transmitting capacity of the actuator.

Wall thickness (mm)	Pressure (kPa)			
	25	50	75	100
1.5	0.43	0.602	1.073	1.602
3.0	0.853	1.485	2.234	2.884
4.5	1.434	2.745	2.835	4.482
6.0	1.743	3.394	4.402	6.423

CONCLUSION

The following conclusions have been drawn from this investigation on the performance of RTV-2 silicone rubber for a cylindrical soft actuator.

i. The elongation behaviour of the actuator is exponential for wall thickness up to 4.5 mm and beyond this thickness, the actuators show a linear elongation. The elongation behaviour is also dependent on the inflation pressure. For any constant wall thickness, the lower inflation pressure results in linear elongation and this trend changes to an exponential with an increase in the inflation pressure.

ii. The numerical simulations and experimental results showed good agreement in axial elongation of the actuator with a maximum error of 14.49 %.

iii. The change in wall thickness from 1.5 mm to 6 mm caused the elongation to reduce by 76.97%, 38.35%, 21.05% and 11.43% at the pressure of 100 kPa, 75 kPa, 50 kPa and 100 kPa respectively. The induced stress was also reduced by 89.61%, 86.66%, 84.46% and 68.68% at these pressures.

iv. The average load-carrying capacity of the actuator is directly proportional to its wall thickness and inflation pressure.

ACKNOWLEDGEMENT

The authors wish to gratefully acknowledge Manipal Academy of Higher Education for providing computational and laboratory facilities.

REFERENCES

[1] O'Neill CT, Phipps NS, Cappello L, Paganoni S, Walsh CJ. A soft wearable robot for the shoulder: design, characterisation, and preliminary testing. In: International Conference on Rehabilitation Robotics, London, UK, pp. 1672-1678; 2017.

[2] Tiboni M, Borboni A, Faglia R, Pellegrini N. Robotics rehabilitation of the elbow based on surface electromyography signals. Advances in Mechanical Engineering 2018; 10(2): 1-14.

[3] Majidi C. Soft Robotics: A Perspective- current trends and prospects for the future. Soft robotics 2013; 1(1): 5-11.

[4] Harvard Biodesign Lab. Retrieved from https://biodesign.seas.harvard.edu/soft-exosuits;1 February, 2019.

[5] Udupa G, Sreedharan P, Dinesh PS, Kim D. Asymmetric bellow flexible pneumatic actuator for miniature robotic soft gripper. Journal of Robotics 2014:1-12.

[6] Robertson MA, Sadeghi H, Florez JM, Paik J. Soft pneumatic actuator fascicles for high force and reliability. Soft Robotics 2017; 4(1): 23-32.

[7] Tolley MT, Shepherd RF, Mosadegh B, Galloway KC et al. A resilient, untethered soft robot. Soft Robotics 2014; 1(0):1-11.

[8] Feng N, Daniel R, Kai T, Lilong C, Tamim A. A jumping robot using soft pneumatic actuator. In: IEEE International Conference on Robotics and Automation, USA, pp 3154-3159; 2015.

[9] Andrew DM, Robert KK, Daniela R. A recipe for soft fluidic elastomer robots. Soft Robotics 2015; 2(1): 7-25.

[10] Giovanni S, Francesco R, Laura S, Lucia RQ. Resistive flex sensors: a survey. Smart Materials and Structures 2016; 25:1-30.

[11] Zhong S, Juan Y, Xiaodong L, Mark HPL, Michael ZQ Chen, Yong H, Zheng W. A soft stretchable bending sensor and data glove applications. Robotics and Biomimetics 2016; 3(1): 22, 1-8.

[12] Merve A, Chansu S, Amir F, Philippe P, Christos I, Charles B, Jamie KP. Sensor Embedded Soft pneumatic actuator for an Endonasal Instrument. In : Proceedings of International Conference on Robotics and Automation, Hong Kong, China, pp. 1-6; 2014.

[13] Panagiotis P, Zheng W, Overvelde TB et al. Modeling of soft fiber-reinforced bending actuators. In: IEEE Transactions on Robotics 2015; 31(3); 778-789.

[14] Yahya E, Augusto V, Constantina L et al. Finite element analysis and design optimization of a pneumatically actuating silicone module for robotic surgery applications. Soft Robotics 2014; 1(4): 255-262.

[15] Moseley P, Florez JM, Sonar HA et al. Modeling, design, and development of soft pneumatic actuators with finite element method. Advanced Engineering Materials 2016; 18(4): 978-988. doi :10.1002/adem.201500503.

[16] Runge G, Wiese M, Gunther L, Raatz A. A framework for the kinematic modeling of soft material robots combining finite element analysis and piecewise constant curvature kinematics. In : 3rd International Conference on Control, Automation and Robotics, Nagoya, Japan, pp. 7-14; 2017.

[17] Frederick L, Valerian V, Eulalie C, Mario SL, Jeremie D, Christian D. Real-time control of soft-robots using synchronous finite element modeling. Proceedings of IEEE International Conference on Robotics and Automation (ICRA), Seattle, WA, 2015; 2550-2555.

[18] Yufei H, Tianmiao W, Ziyu R, Zheyuan G, Hui W, Xingbang Y, Shaoya G, Li W. Modeling and experiments of a soft robotic gripper in amphibious environments. International Journal of Advanced Robotic Systems 2017; 14(3):1-12.

[19] Maria P, Eder M, Raphael D, Monica M et al. Efficient FEM-based simulation of soft robots modeled as kinematic chains. In : Proceedings of IEEE International Conference on Robotics and Robotics, Brisbane, Australia; 2018.

[20] Kit HL, Martin CWL, Marco CK Chow, Hing CF et al. FEM-based soft robotic control framework for intracavitary navigation. In : Proceedings of IEEE International Conference on Real Time Computing and Robotics, Okinawa, 2017, pp. 11-16.

[21] Guanjun B, Lingfeng C, Yaqi Z, Shibo C et al. Trunk-like soft actuator: Design, modeling, and experiments, Robotica 2019;1-15

[22] Wenbin C, Caihua X, Chenlong L, Peimin L, Yonghua C. Fabrication and dynamic modeling of bidirectional bending soft actuator integrated with optical waveguide curvature sensor. Soft Robotics 2019; 6(4): 1-12.

[23] Renato G, Miles M, Xuan L, Yinan S et al. A validated physical model for real-time simulation of soft robotic snakes. International Conference on Robotics and Automation (ICRA), Palais des congres de Montreal, Canada 2019; 6272- 6279.

[24] Weiping H, Rahim M, Weihua L, Gursel A. A structural optimisation method for a soft pneumatic actuator, Robotics 2018; 7(24):1-16:

[25] Ramin Z. Dissipative particle dynamics simulation of the soft micro actuator using polymer chain displacement in electro-osmotic flow, Molecular Simulation 2019: 45(18): 1488-1497.

[26] Fanghao Z, Mingqi Z, Xunuo C, Zhen Z et al. Fabrication and modeling of dielectric elastomer soft actuator with 3D printed thermoplastic frame, Sensors and Actuators: A. Physical 2019: 292 :112-120.

[27] Deepak D, Ameen M, Rohit J, Kashish K. Studies on development of soft robotic bending actuator using natural rubber. Indian Journal of Science and Technology 2016; 9(42):1 - 4.

[28] Cantournet S, Desmorat R, Besson J. Mullins effect and cyclic stress softening of filled elastomers by internal sliding and friction thermodynamics model. International Journal of Solids and Structures 2009; 46(11-12):2255-2264.